Thermo-optic control of dielectric-loaded plasmonic waveguide components

Jacek Gosciniak[1], Sergey I. Bozhevolnyi[1,*], Thomas B. Andersen[1], Valentyn S. Volkov[1], Jakob Kjelstrup-Hansen[2], Laurent Markey[3], and Alain Dereux[3]

[1]*Institute of Sensors, Signals and Electrotechnics (SENSE), University of Southern Denmark, Niels Bohrs Allé 1, DK-5230 Odense M, Denmark*
[2]*NanoSYD, Mads Clausen Institute, University of Southern Denmark, Alsion 2, DK-6400 Sønderborg, Denmark*
[3]*Institut Carnot de Bourgogne, UMR 5209 CNRS-Université de Bourgogne, 9 Av. A. Savary, BP 47 870, F-21078 Dijon Cedex, France*
** seib@sense.sdu.dk*

Abstract: We report preliminary results on the development of compact (length < 100 μm) fiber-coupled dielectric-loaded plasmonic waveguide components, including Mach-Zehnder interferometers (MZIs), waveguide-ring resonators (WRRs) and directional couplers (DCs), whose operation at telecom wavelengths is controlled via the thermo-optic effect by electrically heating the gold stripes of dielectric-loaded plasmonic waveguides. Strong output modulation (> 20%) is demonstrated with MZI- and WRR-based components, and efficient (~30%) rerouting is achieved with DC switches.

OCIS codes: (240.6680) Surface plasmons; (250.5300) Photonic integrated circuits

References and links

1. *Plasmonic Nanoguides and Circuits*, S. I. Bozhevolnyi, ed. (Pan Stanford Publishing, Singapore, 2008).
2. T. W. Ebbesen, C. Genet, and S. I. Bozhevolnyi, "Surface-plasmon circuitry," Phys. Today **61**(5), 44–50 (2008).
3. T. Nikolajsen, K. Leosson, and S. I. Bozhevolnyi, "Surface plasmon polariton based modulators and switches operating at telecom wavelengths," Appl. Phys. Lett. **85**(24), 5833–5835 (2004).
4. G. Gagnon, N. Lahoud, G. A. Mattiussi, and P. Berini, "Thermally activated variable attenuation of long-range surface plasmon-polariton waves," J. Lightwave Technol. **24**(11), 4391–4402 (2006).
5. M. J. Dicken, L. A. Sweatlock, D. Pacifici, H. J. Lezec, K. Bhattacharya, and H. A. Atwater, "Electrooptic modulation in thin film barium titanate plasmonic interferometers," Nano Lett. **8**(11), 4048–4052 (2008).
6. J. A. Dionne, K. Diest, L. A. Sweatlock, and H. A. Atwater, "PlasMOStor: a metal-oxide-Si field effect plasmonic modulator," Nano Lett. **9**(2), 897–902 (2009).
7. D. Pacifici, H. J. Lezec, and H. A. Atwater, "All-optical modulation by plasmonic excitation of CdSe quantum dots," Nat. Photonics **1**(7), 402–406 (2007).
8. R. A. Pala, K. T. Shimizu, N. A. Melosh, and M. L. Brongersma, "A nonvolatile plasmonic switch employing photochromic molecules," Nano Lett. **8**(5), 1506–1510 (2008).
9. K. F. MacDonald, Z. L. Sámson, M. I. Stockman, and N. I. Zheludev, "Ultrafast active plasmonics," Nat. Photonics **3**(1), 55–58 (2009).
10. T. Holmgaard, and S. I. Bozhevolnyi, "Theoretical analysis of dielectric-loaded surface plasmon-polariton waveguides," Phys. Rev. B **75**(24), 245405 (2007).
11. A. V. Krasavin, and A. V. Zayats, "Passive photonic elements based on dielectric-loaded surface plasmon polariton waveguides," Appl. Phys. Lett. **90**(21), 211101 (2007).
12. T. Holmgaard, S. I. Bozhevolnyi, L. Markey, and A. Dereux, "Dielectric-loaded surface plasmon-polariton waveguides: Excitation and characterization," Appl. Phys. Lett. **92**(1), 011124 (2008).
13. T. Holmgaard, Z. Chen, S. I. Bozhevolnyi, L. Markey, A. Dereux, A. V. Krasavin, and A. V. Zayats, "Wavelength selection by dielectric-loaded plasmonic components," Appl. Phys. Lett. **94**(5), 051111 (2009).
14. Z. Chen, T. Holmgaard, S. I. Bozhevolnyi, A. V. Krasavin, A. V. Zayats, L. Markey, and A. Dereux, "Wavelength-selective directional coupling with dielectric-loaded plasmonic waveguides," Opt. Lett. **34**(3), 310–312 (2009).
15. J. Grandidier, G. C. des Francs, S. Massenot, A. Bouhelier, L. Markey, J.-C. Weeber, C. Finot, and A. Dereux, "Gain-assisted propagation in a plasmonic waveguide at telecom wavelength," Nano Lett. **9**(8), 2935–2939 (2009).
16. J. Gosciniak, V. S. Volkov, S. I. Bozhevolnyi, L. Markey, and A. Dereux, "Fiber-coupled dielectric-loaded plasmonic waveguides," Appl. Phys. Lett. submitted.
17. T. Holmgaard, S. I. Bozhevolnyi, L. Markey, A. Dereux, A. V. Krasavin, P. Bolger, and A. V. Zayats, "Efficient excitation of dielectric-loaded surface plasmon-polariton waveguide modes at telecommunication wavelengths," Phys. Rev. B **78**(16), 165431 (2008).
18. M. J. Weber, *Handbook of Optical Materials* (CRC Press, New York, 2003).

#120750 - $15.00 USD Received 30 Nov 2009; revised 31 Dec 2009; accepted 2 Jan 2010; published 8 Jan 2010

19. T. Holmgaard, Z. Chen, S. I. Bozhevolnyi, L. Markey, and A. Dereux, "Design and characterization of dielectric-loaded plasmonic directional couplers," J. Lightwave Technol. **27**(24), 5521–5528 (2009).

1. Introduction

Photonic components utilizing surface plasmon polaritons (SPPs) have been intensively investigated for diverse applications, including their usage for the development of ultracompact photonic circuits [1]. To be complete, plasmonic circuits should incorporate active components capable of modulating the transmitted field phase and/or amplitude as well as rerouting radiation between optical channels [2]. Implementation of SPP modulation is strongly influenced by the strength of material effects available, such as thermo-, electro- and magneto-optical effects or optical nonlinearities (for all-optical radiation control). However, since these effects are inherently weak and SPP propagation is rather limited by inevitable SPP absorption losses, the challenge faced when attempting to realize SPP modulation is enormous. Long-range SPP-based thermo-optical modulators and switches (with efficient fiber in- and out-coupling of radiation) were the first plasmonic components in which the same metal circuitry was used to both guide the optical radiation and transmit the electrical signals that efficiently control the guidance [3, 4]. Recently, the electro-optic modulation in thin-film interferometers supporting the SPP propagation [5] and the electrical control of light transmission with a field effect Si modulator based on multimode interference in a plasmonic waveguide [6] were realized as well as efficient all-optical modulation of SPP transmission via influencing absorption in dielectric (by embedded quantum dots [7] and photochromic molecules [8]) and metal [9]. It should be stressed that, in the above cases [5–9], the modulation was achieved using essentially *planar* SPP modes, i.e. not confined in the lateral direction, whose excitation and detection required elaborate instrumental arrangements.

Among various SPP-based waveguide configurations [1, 2], dielectric-loaded SPP waveguides (DLSPPWs) [10, 11] represent an attractive alternative by virtue of being naturally compatible with different dielectrics and industrial fabrication using large-scale UV lithography [12]. DLSPPWs have already been found suitable for realization of *passive* photonic devices, including ultracompact wavelength-selective components [13, 14]. Furthermore, gain-assisted SPP propagation in DLSPPWs has very recently been demonstrated by doping the DLSPPW polymer layer with quantum dots whose stimulated emission resulted in a noticeable (~27%) increase of mode propagation length [15]. However, their potential for *active* modulation of transmitted fields has so far not been explored. In the present work we report *preliminary* results on the development of *fiber-coupled* DLSPPW-based components, including Mach-Zehnder interferometers (MZIs), waveguide-ring resonators (WRRs) and directional couplers (DCs), whose operation at telecom wavelengths is *actively* controlled via the thermo-optic effect by electrical signals transmitted through the *same* gold stripes that support dielectric (polymer) ridges of DLSPPWs. The main idea is to advantageously exploit the circumstance that the DLSPPW mode field reaches its maximum at the metal-dielectric interface and thereby at the heating electrode, unlike in most conventional dielectric waveguides, where the mode power extends far out in the surrounding cladding and the proximity of electrodes should be avoided to minimize the absorption loss.

All investigated DLSPPW-based components were fabricated by deep UV lithography (wavelength of ~250 nm) with a Süss Microtech MJB4 mask aligner in the vacuum contact mode and using consecutively two (commercial) masks, first to pattern a 50-nm-thick gold film deposited on a (~750-μm-thick) magnesium fluoride (MgF_2) substrate and then to define dielectric (polymer) ridges of the DLSPPW circuitry using a spin-coated (~1-μm-thick) layer of poly-methyl-methacrylate (PMMA) resist. The fabricated sample contained various DLSPPW-based components (including straight waveguides, MZIs, WRRs and DCs) placed parallel to each other, with PMMA ridges being ~1-μm-wide in principal regions of the components. These narrow ridges were on both sides connected via 25-μm-long funnel structures with access (10-μm-wide) polymer waveguides extending *outside* gold covered regions of DLSPPWs all the way up to the substrate edges (Fig. 1), facilitating thereby the end-fire coupling of access ridge waveguides (ARWs) with single-mode optical fibers (core

#120750 - $15.00 USD Received 30 Nov 2009; revised 31 Dec 2009; accepted 2 Jan 2010; published 8 Jan 2010

diameter ~10 μm). In passing we note that the MgF_2 substrates were chosen because of their low refractive index (~1.37), which was required to ensure efficient guiding by ARWs. The final fabrication step was a cleavage of the sample perpendicular to the ARWs resulting in ~2-mm-long and ~10-μm-wide polymer ARWs leading toward each side of the DLSPPW area. It should be noted that, unfortunately, the edge quality of the cleaved sample was found to be varying between different ARWs leading to different DLSPPW-based components, strongly influencing the level of coupling losses in the fiber-to-fiber transmission measurements.

2. Fiber-DLSPPW-fiber transmission

Characterization of the fiber-to-fiber coupling efficiency has been carried out for straight DLSPPWs using standard transmission measurements with a tunable laser (wavelength range of 1450 – 1600 nm) as a radiation source and an optical spectrum analyzer (OSA) as a detector. TM/TE-polarized laser radiation (the electric field is perpendicular/parallel to the sample surface plane) was launched into the input ARWs via end-fire coupling from a polarization-maintaining (PM) single-mode fiber (Fig. 1). The adjustment of the in-coupling fiber with respect to the input ARW was accomplished by monitoring the output facet of the sample with the help of a far-field microscopic arrangement (with an IR-Vidicon camera and a properly adjusted 50× microscope objective). It was observed that for a 1-μm-thick and 10-μm-wide ARW, the mode field diameter is symmetric and well matched to that of a standard PM single-mode fiber used in our experiments. The far-field observations have also confirmed the expected polarization properties of the DLSPPW mode [10], i.e. the efficient coupling of the ARW modes into DLSPPs has been found only with TM-polarized radiation, and revealed a relatively low level of the total insertion loss. Following these experiments (that include also adjusting the in-coupling fiber position to maximize the coupling efficiency) we replaced the far-field microscopic arrangement with another PM single-mode fiber that was used to collect the out-coupled power and to send it to an OSA.

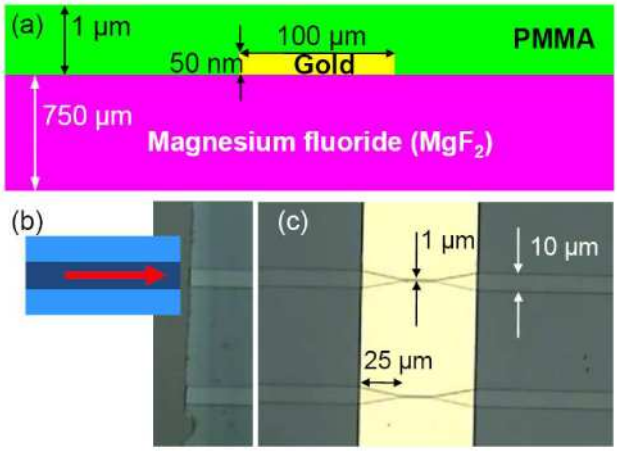

Fig. 1. (a) Schematic cross section of straight DLSPPWs integrated with ARWs. Optical microscope images showing top views: (b) a fragment of the cleaved sample edge with the in-coupling fiber drawn schematically (not to scale) and (c) the central part of the sample that features a 100-μm-wide gold stripe with straight DLSPPWs connected via funnels to input/output ARWs.

We have conducted detailed investigations of the fiber-to-DLSPPW coupling via ARWs in this configuration [16] with the most relevant results as follows. The transmission spectra recorded in the wavelength range from 1450 to 1600 nm with the OSA sensitivity of –80 dBm for straight DLSPPWs revealed that, in general, the transmission for different DLSPPWs exhibited similar wavelength dependences with the maximum transmission being detected at the wavelength of ~1480 nm, gradually deteriorating for both longer and shorter wavelengths. Since the DLSPPW propagation loss decreases monotonously for longer wavelengths [17],

#120750 - $15.00 USD Received 30 Nov 2009; revised 31 Dec 2009; accepted 2 Jan 2010; published 8 Jan 2010

we believe that this maximum should be attributed to the realization of optimum conditions for the ARW-DLSPPW coupling. The overall, i.e. fiber-to-fiber, insertion loss was found to be at the level of ~24 dB for the wavelength range of 1460-1570 nm. Taking into account the propagation loss (~12 dB at $\lambda \approx 1550$ nm) calculated for 100-μm-long DLSPPWs [10, 17], one obtains ~6 dB for the fiber-ARW and ARW-DLSPPW coupling losses together, a value that seems reasonable considering the mode field mismatches at these two interfaces (as was also confirmed by simple calculations of the corresponding overlap integrals [16]). It should also be noted, that the fiber-ARW coupling loss can be significantly decreased by use of the in-coupling fiber with a smaller (~4 μm) core diameter. Some improvement is also expected for the ARW-DLSPPW coupling when properly adjusting the PMMA thickness.

3. Mach-Zehnder interferometric modulators

The MZI configuration represents probably the most amenable and straightforward waveguide arrangement for the intensity modulation of transmitted radiation [3]. The generic operation principle of MZI modulator is as follows. In the absence of a control signal, an input optical wave is split equally into two waves travelling along two identical MZI arms that are again joined together producing an output wave. Ideally, the two waves meeting in the output junction are identical in phase and amplitude. When a control signal is applied to one of the MZI arms, the propagation of the corresponding wave is influenced (via one of the optical material effects), causing its phase to lag so that the phases of two recombining waves are different at the output junction, resulting in a decrease of the MZI output. In our case (Fig. 2), the operation of a thermo-optic MZI modulator is based on changing the DLSPPW propagation constant in a heated arm resulting in the phase difference of two DLSPPW modes that interfere in the output Y-junction. The length of the heated MZI arm required to ensure the complete modulation is given by $L_\pi = \lambda/(2\Delta T_{max}|\partial n/\partial T|)$, where λ is the light wavelength in vacuum, ΔT_{max} is the maximum change in temperature determined, essentially, by the difference in the glass temperature of polymer used and the ambient temperature, $\gamma = |\partial n/\partial T|$ is the magnitude of the thermo-optic coefficient [3]. Considering PMMA, i.e., $\gamma \cong 1.05 \cdot 10^{-4}$ $^\circ K^{-1}$ and $\Delta T_{max} \cong 65^\circ K$ (as estimated from the maximum service temperature of 360°K [18]), one obtains $L_\pi \cong 113.5$ μm for $\lambda = 1.55$ μm.

The MZI modulators (fabricated on the same substrate simultaneously with straight DLSPPWs considered above) were 115-μm-long in total, including two 25-μm-long funnels, two 5-μm-long and 1-μm-wide straight DLSPPW sections connecting the funnels and the MZI arms split (and joined) by two 10-μm-long S-bends, the parallel 35-μm-long sections of MZI arms being separated by 8 μm [Fig. 2(a)]. The gold film was patterned so that gold stripes could be used both as supports of DLSPPWs and electrodes allowing for heating (with electrical currents) one MZI arm that was electrically isolated with 1.5-μm-wide gaps. These gaps might introduce additional scattering loss that is yet to be quantified. Ultrasonic wire bonding was used to connect aluminum wires to ~200-μm-wide and 500-μm-long bonding pads of the MZI modulator on the sample substrate and pre-structured electrodes on a carrier substrate. The overall resistance was measured to be ~25 Ω, with the heating (4-μm-wide) electrode resistance being evaluated as ~5 Ω [4, 18]. Note that the length of the heated MZI arm was only $L \cong 41$ μm [Fig. 2(a)], which is nearly 3 times smaller than L_π calculated above. The choice of such an arm length was impelled by considerations of the trade-off between the modulation efficiency expected and the propagation loss incurred in DLSPPWs (typical propagation length of radiation in DLSPPWs is ~60 μm), bearing in mind also that the *primary* goal of this work was to demonstrate the thermo-optic modulation with DLSPPWs.

#120750 - $15.00 USD Received 30 Nov 2009; revised 31 Dec 2009; accepted 2 Jan 2010; published 8 Jan 2010

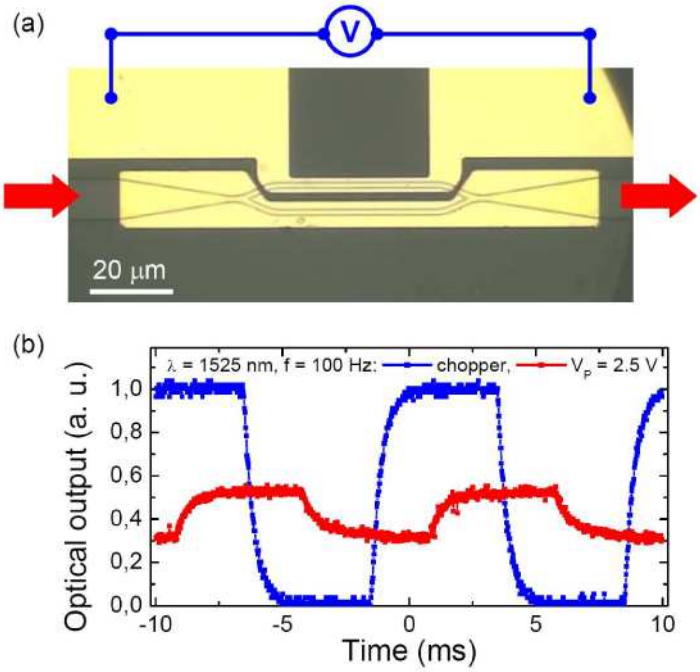

Fig. 2. (a) Optical microscope image showing the main part of MZI modulator with connecting electrodes drawn schematically (not to scale) and (b) its temporal response (red) measured at the frequency of 100 Hz with an offset of 1.25 V and a peak-to-peak voltage of 2.5 V. For comparison, the MZI output signal when the input light was chopped externally is also shown in (b).

We have conducted fiber-to-fiber transmission characterization of the DLSPPW-based MZI modulators as described in Section 2 except for using (instead of OSA) a fiber-pigtailed femtowatt InGaAs photoreceiver. External mechanical modulation of laser output by a chopper was used for the calibration of the modulation depth (the induced change in the transmitted optical power related to the unperturbed optical output) achieved with our thermo-optically controlled components [Fig. 2(b)]. It was found that the modulation depth exceeding 20% could be achieved as was actually expected, since the estimate of maximum modulation in the current configuration amounted to $\eta_{max} \cong \sin^2(\pi\gamma L\Delta T_{max}\lambda^{-1})$ ~0.3. However, the electrical power required was unexpectedly high (~0.25 W) whereas the temporal response was very slow [Fig. 2(b)]. Both these features are related to rather "unfortunate" thermal properties of MgF_2 substrate, whose thermal conductivity is 130 times (!) larger than that of PMMA [18]. This circumstance entails that the main heat dissipation occurring when the external voltage is applied to the electrodes takes place in the substrate, whose thermal capacity is practically unlimited. Here, we have to emphasize that our choice of the substrate material was dictated by the availability of MgF_2 substrates that have a sufficiently low refractive index (~1.37), which is in turn required to ensure efficient guiding by ARWs [16] whose usage is *indispensible* for the realization of fiber-to-fiber transmission characterization (as opposed to near-field imaging employed in the previous experiments with the DLSPPW-based components [12–14]). In the *opposite* limit of the thermal conductivity of a substrate being negligibly small as compared to that of PMMA, one obtains the following estimate for the driving power [3]: $P_\pi \sim 0.5\ (\kappa\lambda/\gamma)w/d \approx 1.4$ mW, where κ ~0.2 W/mK is the PMMA thermal conductivity [18], w and d are the PMMA ridge width and height: $w \approx d \approx 1\ \mu$m. Under the same conditions, the corresponding time constant can also be estimated in a simple manner [3], resulting in $\tau \sim c_\rho \rho\, d^2/\kappa \approx 5\ \mu$s, where c_ρ ~1 J/gK is the specific heat capacitance and ρ ~1 g/cm^3 is the specific mass density of PMMA [18]. These estimations reveal a great potential

#120750 - $15.00 USD Received 30 Nov 2009; revised 31 Dec 2009; accepted 2 Jan 2010; published 8 Jan 2010

of DLSPPW-based thermo-optic components that can be developed into practical plasmonic components with superior characteristics.

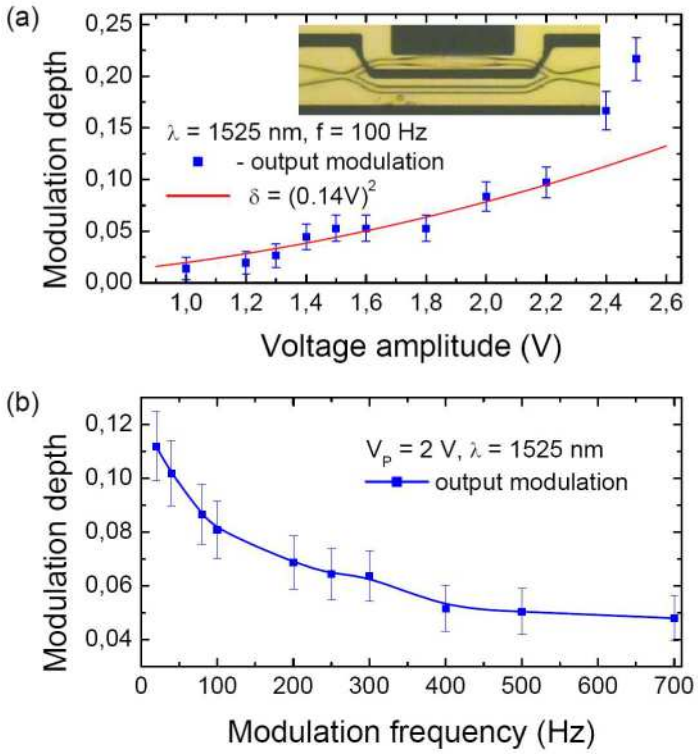

Fig. 3. Dependences of MZI depth modulation (a) on the applied voltage amplitude with inset showing the thermal damage of an overheated (by electrical currents) MZI arm and (b) on the modulation frequency (solid curve shows a spline approximation of data to guide the eye).

Using fiber-to-fiber transmission measurements we have investigated the modulation depth dependences on the applied (at the frequency of 100 Hz) voltage amplitude [Fig. 3(a)] and on the modulation (with the peak-to-peak voltage of 2 V) frequency [Fig. 3(b)] for the fabricated MZI modulators. It is seen that an approximately quadratic dependence of the modulation depth on the applied voltage (as expected for small phase lags induced) becomes strongly nonlinear for larger voltage amplitudes, resulting eventually in the thermal damage of a PMMA ridge of MZI arm [Fig. 3(a)] occurring for electrical currents of ~100 mA. The frequency dependence of the modulation depth [Fig. 3(b)] exhibits a drastic decrease even for very low frequencies because the substrate heating by an MZI electrode is extremely slow as will be shown below. However, for relatively large frequencies, the decrease slows down indicating the transition to the regime in which the substrate heating cannot follow rapid variations in the applied voltage. In this case, the modulated electrical current influences only the heating of a PMMA ridge of MZI arm, a process which is relatively fast but extremely inefficient as discussed above. Finally, it should be noted that the investigated DLSPPW-based MZI modulators exhibited, as expected, very similar characteristics for other telecom wavelengths than that specified in Figs. 2 and 3.

4. Waveguide-ring resonators

The thermo-optic modulation of transmission with DLSPPW-based WRRs can be considered essentially in the same manner as that realized with DLSPPW-based MZIs discussed in the previous section. The main difference is related to the fact that, contrary to MZIs, the WRR transmission depends strongly on the wavelength used exhibiting a periodic dependence with

#120750 - $15.00 USD Received 30 Nov 2009; revised 31 Dec 2009; accepted 2 Jan 2010; published 8 Jan 2010

respect to the phase accumulated by the ring-DLSPPW mode per circulation [13]. This means that, depending on the wavelength, the heating of WRR ridges can cause an increase or decrease in the WRR transmission, because a thermally induced phase lag of the ring-DLSPPW mode can bring this mode closer or farther away from the condition of constructive interference with the DLSPPW mode (of a straight waveguide) entering the coupling region. In that respect, a change in ridge temperature, causing a change in its refractive index, produces a *similar*, to a change in the light wavelength, effect on the WRR transmission. The WRR modulators (fabricated simultaneously with the MZI modulators and in the same fashion) contained 5-μm-radius ring resonators placed with a ~0.5-μm-wide gap near 30-μm-long and 1-μm-wide straight DLSPPW sections connected to 25-μm-long funnels [Fig. 4(a)]. The gold film was patterned so as to ensure the heating (with 4-μm-wide electrodes) of both ring resonators and coupling sections, avoiding thereby the usage of (demanding careful fabrication) narrow gaps in the electrode system (as was needed in the design of MZI modulators [cf. Figures 2(a) and 4(a)]) as well as large temperature variations in the coupling region that might otherwise introduce additional scattering losses.

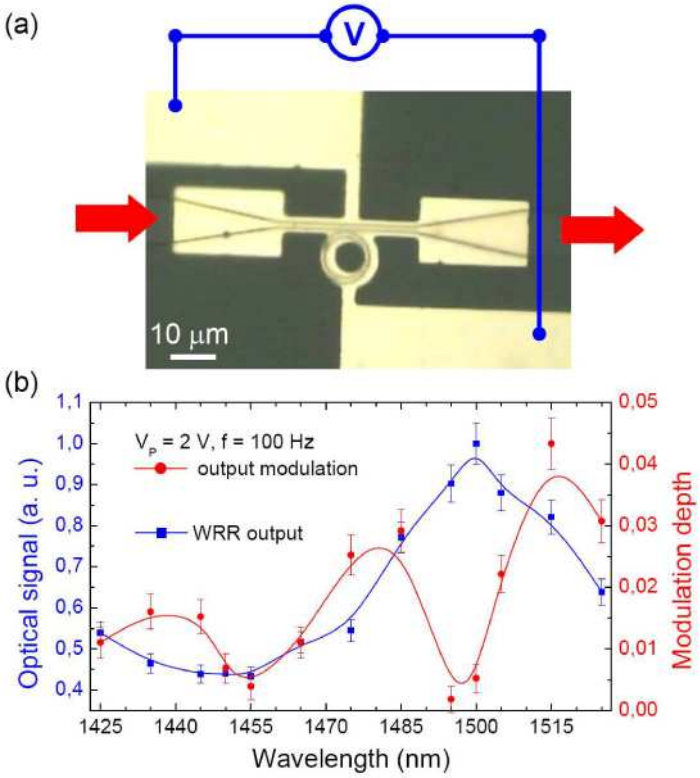

Fig. 4. (a) Optical microscope image showing the main part of WRR modulator with connecting electrodes drawn schematically (not to scale) and (b) the wavelength dependences of WRR transmission (measured without an applied voltage) and modulation depth measured with an offset of 1 V and a peak-to-peak voltage of 2 V at the modulation frequency of 100 Hz (solid curves show spline approximations of data sets to guide the eye).

In our investigations of the fabricated WRR modulators, we first measured the WRR transmission as a function of the light wavelength in the absence of applied electrical currents [Fig. 4(b)]. It was found that the wavelength dependence was more complicated and less pronounced than observed previously [13]. We relate this behavior to the circumstance that we used in these experiments slightly wider and taller PMMA ridges than in our previous investigations, exceeding actually the upper limit of single-mode DLSPPW operation [10]. Our choice of current DLSPPW parameters was aimed at improving the field matching at the

#120750 - $15.00 USD Received 30 Nov 2009; revised 31 Dec 2009; accepted 2 Jan 2010; published 8 Jan 2010

ARW-DLSPPW transition and thereby at decreasing the overall insertion loss [16]. Another reason for this unexpected wavelength dependence of WRR transmission might be related to misalignment (occurred during the fabrication) between the gold and PMMA rings [Fig. 4(a)] causing unusual dispersion of the ring-DLSPPW mode [13].

In the next step we measured the wavelength dependence of modulation depth using moderate applied voltage and modulation frequency [Fig. 4(b)]. It is seen that the modulation dependence obtained oscillates faster, by approximately two times, than the transmission dependence, reaching maxima at linear slopes of the latter, a feature which should have been in fact expected due to the aforementioned similarity (in WRR transmission response) between changing the WRR temperature and tuning the light wavelength. The maximum modulation efficiency observed was ~10%, a value which is consistent with the WRR ring circumference of ~31 μm (~4 times shorter than L_π) and a relatively low contrast in the measured WRR transmission dependence on the light wavelength [Fig. 4(b)]. The latter can be significantly improved by adjusting the DLSPPW parameters to ensure the single-mode operation and by optimizing the waveguide-ring gap, which is the most crucial parameter responsible for the waveguide-ring coupling strength [13]. Finally, we would like to note that it was also observed that the dependences of WRR depth modulation on the applied voltage amplitude and on the modulation frequency (not shown here) were quite similar to those measured for the MZI modulators (Fig. 3).

5. Directional couplers

The thermo-optic rerouting of radiation with DLSPPW-based DC switches turned out to be considerably more difficult to realize, because it was practically impossible to follow the approach developed for long-range SPP-based directional couplers [3], in which one of two coupled waveguides was selectively heated introducing the phase mismatch between the coupled modes and changing thereby the output power allocation between these waveguides. In the case of DLSPPWs, a metal stripe supporting a dielectric ridge should be sufficiently wide in order to prevent the interaction between the DLSPPW mode field and the stripe edges that might instigate additional (radiation and scattering) mode losses. On the other hand, efficient coupling in DLSPPW-based DCs requires submicron separations between the dielectric ridges [19], a requirement that *cannot* be met simultaneously with the preceding one when implementing *separate* heating of coupled DLSPPWs. We circumvented this problematic issue by making use of the wavelength sensitivity of DLSPPW-based DCs that can be tuned by dedicated design [14, 19]. As in the case of WRRs, the DC transmission sensitivity with respect to the light wavelength implies that the DC transmission can be influenced by changing the temperature of ridges, causing changes in their refractive indexes, i.e. that the thermo-optic rerouting of radiation can be achieved by heating *simultaneously* both coupled DLSPPWs. Clearly, as compared to *separate* heating of waveguides [3], this approach relies on a much weaker, second-order, effect that has yet to be theoretically analyzed and considered from the point of view of its optimization.

Leaving detailed considerations of this configuration for future studies, we present in the following only preliminary experimental results obtained when examining the above idea. The DC switches (fabricated simultaneously with the MZI and WRR modulators and in the same fashion) contained 20-μm-long coupling (zero-gap separation) sections connecting on both sides to 10-μm-long and 7-μm-offset S-bends leading (via 5-μm-long straight DLSPPW sections) to the funnels having the same parameters as those employed in MZI and WRR modulators [Fig. 5(a)]. These funnels were connected with the ARWs extending outside gold covered regions all the way up to the substrate edges, so that the direct and coupled signals could be measured by imaging the corresponding ARW output edge on a photoreceiver. The gold film was patterned so as to ensure the heating with 6-μm-wide electrodes of the coupling sections but, in contrast to the WRR electrode configuration, the heating electrodes were electrically isolated (with 2-μm-wide gaps) from the rest of gold support of DLSPPW-based DCs [cf. Figures 4(a) and 5(a)]. The overall length of heated coupling section was therefore

#120750 - $15.00 USD Received 30 Nov 2009; revised 31 Dec 2009; accepted 2 Jan 2010; published 8 Jan 2010

only 16 μm, so that it was expected that the DC switches would be less efficient than the MZI and WRR modulators and rather slow because of wider heating electrodes.

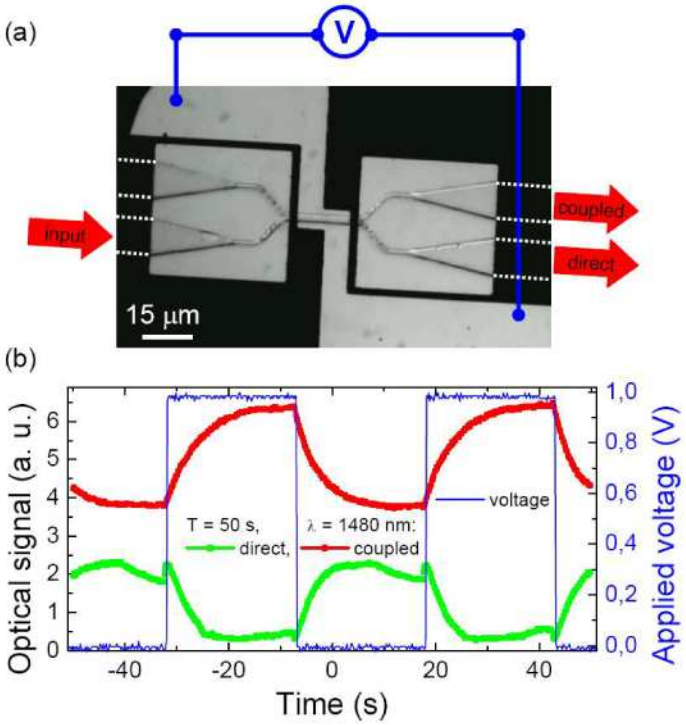

Fig. 5. (a) Optical microscope image showing the main part of DC switch with connecting electrodes drawn schematically (not to scale) and ARWs indicated by white dotted lines. (b) The DC switch output signal temporal responses in the direct (green) and coupled (red) channels measured at the frequency of 20 mHz with an offset of 0.5 V and a peak-to-peak voltage of 1 V. The voltage applied to the DC electrodes is also shown in (b).

Bearing the above considerations in mind, we subjected the fabricated DC switches to very low-frequency modulation, i.e. with the period of 50 s, and simply tuned the wavelength until the output optical signals exhibited well-pronounced temporal responses [Fig. 5(b)]. The observed time constant of ~10 s (that should be attributed to substrate heating) accounts for the frequency response reported for the MZI modulators [Fig. 3(b)]. The switching efficiency being of ~30% for the modulation period of 50 s decreased rapidly with the modulation frequency increase, so that measurements at frequencies higher than 200 Hz could not be reliably carried out. We consider the preliminary results obtained encouraging enough to warrant further investigations of this switching configuration complementing experiments with theoretical modeling and numerical simulations.

6. Conclusion

Compact fiber-coupled DLSPPW-based components, including MZIs, WRRs and DCs, whose outputs were controlled via the thermo-optic effect by electrically heating the gold stripes supporting polymer ridges of DLSPPWs have been designed, fabricated and characterized at telecom wavelengths using fiber-to-fiber transmission measurements. Our preliminary experiments have shown strong output modulation (> 20%) obtained with MZI- and WRR-based components and efficient (~30%) rerouting achieved with DC switches. Moreover, our estimations (Section 3) demonstrated that, with a propitious choice of the materials, the performance of these components can be significantly improved, indicating thereby a great potential of DLSPPW-based thermo-optic components that can be used as

#120750 - $15.00 USD Received 30 Nov 2009; revised 31 Dec 2009; accepted 2 Jan 2010; published 8 Jan 2010

compact low-power variable optical attenuators and optical switches and cross-connectors in reconfigurable photonic circuits.

Acknowledgements

This work was supported by EC FP6 STREP PLASMOCOM. The authors thank Zhuo Chen (Nanjing University) for conducting experimental investigations at the initial stage of research into thermo-optically controlled DLSPPW-based components.

#120750 - $15.00 USD Received 30 Nov 2009; revised 31 Dec 2009; accepted 2 Jan 2010; published 8 Jan 2010